

Coherent control of optical four-wave mixing by two-color ω - 3ω ultrashort laser pulses

Carles Serrat

Departament de Física i Enginyeria Nuclear, Universitat Politècnica de Catalunya, Colom 1, 08222 Terrassa, Spain

(Dated: July 26, 2018)

A theoretical investigation on the quantum control of optical coherent four-wave mixing interactions in two-level systems driven by two intense synchronized femtosecond laser pulses of central angular frequencies ω and 3ω is reported. By numerically solving the full Maxwell-Bloch equations beyond the slowly-varying envelope and rotating-wave approximations in the time domain, the nonlinear coupling to the optical field at frequency 5ω is found to depend critically on the initial relative phase ϕ of the two propagating pulses; the coupling is enhanced when the pulses interfere constructively in the center ($\phi = 0$), while it is nearly suppressed when they are out of phase ($\phi = \pi$). The tuning of the initial absolute phase of the different frequency components of synchronously propagating ω - 3ω femtosecond pulses can serve as a means to control coherent anti-Stokes Raman (CARS) processes.

In recent years, encouraged by the developments in the engineering of intense ultrashort laser fields with a well defined absolute phase [1], studies on the phase control of the interaction of two-color strong ultrashort laser pulses in nonlinear materials have received a great interest [2, 3, 4, 5, 6, 7]. Phenomena arising from such ultrashort pulse interaction can be of extreme importance in fields as diverse as optoelectronics and materials research, in biological applications such as spectroscopy and microscopy, in high harmonic generation, and in photoionization or molecular dissociation, among others.

It is known that when the pulses duration approach the duration of only several optical cycles, theories based on the slowly-varying envelope approximation (SVEA) and the rotating-wave approximation (RWA) are not appropriate, since phenomena such as electric field time-derivatives leading to carrier-wave reshaping [8], or the generation of high spectral components [9], can not be described by such theories. In these situations, accurate numerical modeling based on the finite-difference time-domain (FDTD) method [10] is being increasingly used to investigate the full set of optical Maxwell-Bloch equations [7, 8, 9, 11].

In this Letter, we investigate the possibility of phase control of transient four-wave mixing interactions in two-level systems driven by two mutually coherent intense ultrashort pulses of central angular frequencies ω and 3ω . We employ a standard predictor-corrector FDTD numerical approach which incorporates all propagation effects—such as nonlinearity, dispersion, absorption, dissipation, saturation, and other resonance effects— [8], to study the sensitivity on the relative phase ϕ of the nonlinear coupling of the ω - 3ω pulses to the field at frequency 5ω , which results from the interaction of the waves through the third order susceptibility of the medium ($\chi^{(3)}$) [12].

By describing the evolution of the field spectrum as the two-color pulses propagate through the medium, our simulations demonstrate that the generation of the 5ω -component is enhanced when the two pulses are in phase ($\phi = 0$), while it is nearly suppressed when they are out

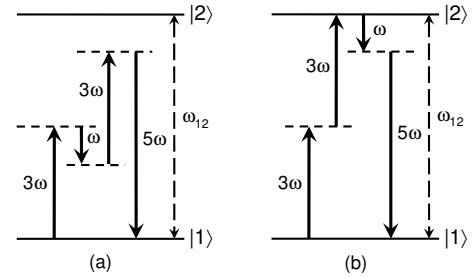


FIG. 1: Schematic energy level diagrams corresponding to the first case of our study. The four-wave mixing can occur between the injected two-color fields at frequencies ω and 3ω , and a third generated field at frequency 5ω , by parametric coupling (a) or by two-photon processes (b). The wavelengths associated to the frequencies in this scheme are: $\lambda_{(\omega)} = 2400$ nm; $\lambda_{(3\omega)} = 800$ nm; $\lambda_{(5\omega)} = 480$ nm; $\lambda_{(\omega_{12})} = 400$ nm. The area of both pulses is $A = 20\pi$.

of phase ($\phi = \pi$). In what follows, we analyze this effect in two different configurations:

– First, we consider a nonresonant case with large pulse intensities (see Fig. 1). The two injected pulses have a duration of 10 fs and they initially overlap in time. The pulse area for both pulses is $A = 20\pi$ [13], and the wavelengths are $\lambda_{(\omega)} = 2400$ nm and $\lambda_{(3\omega)} = 800$ nm. The fields are largely detuned from the atomic transition resonance ($\lambda_{(\omega_{12})} = 2\pi c/\omega_{12} = 400$ nm), although the two-photon coupling of the field with $\lambda_{(3\omega)} = 800$ nm is considered in resonance (see Fig. 1 (b)). Therefore, by four-wave mixing, the fields can interact with a generated third wave with $\lambda_{(5\omega)} = 480$ nm, by either the parametric coupling represented in Fig. 1 (a) or through a two-photon process [Fig. 1 (b)]. We note that the energy level diagrams of this first study can be considered as an example of the vibrational nonresonant contributions at zero pump-probe time delay in CARS processes [14].

– In a second study, we consider two 10 fs pulses with

moderate pulse areas ($A = 4\pi$) and wavelengths as $\lambda_{(\omega)} = 1743$ nm and $\lambda_{(3\omega)} = 581$ nm. In this case, the field with $\lambda_{(3\omega)} = 581$ nm propagates close to resonance with the atomic transition ($\lambda_{(\omega_{12})} = 580$ nm). By a nonlinear third order parametric coupling (see Fig. 5) the fields can produce a wave with $\lambda_{(5\omega)} = 348.6$ nm. The parameter values in this second study have been chosen to be close to those for transitions that are relevant in biological applications, with similar schemes being currently investigated with femtosecond CARS techniques [14, 15, 16].

The Maxwell-Bloch equations can be written as [8]

$$\begin{aligned} \frac{\partial H_y}{\partial t} &= -\frac{1}{\mu_0} \frac{\partial E_x}{\partial z} \\ \frac{\partial E_x}{\partial t} &= -\frac{1}{\epsilon_0} \frac{\partial H_y}{\partial z} - \frac{N_{at}\Gamma}{\epsilon_0 T_2} (\rho_1 - T_2 \omega_{12} \rho_2) \\ \frac{\partial \rho_1}{\partial t} &= -\frac{1}{T_2} \rho_1 + \omega_{12} \rho_2 \\ \frac{\partial \rho_2}{\partial t} &= -\frac{1}{T_2} \rho_2 + \frac{2\Gamma}{\hbar} E_x \rho_3 - \omega_{12} \rho_1 \\ \frac{\partial \rho_3}{\partial t} &= -\frac{1}{T_1} (\rho_3 - \rho_{30}) - \frac{2\Gamma}{\hbar} E_x \rho_2 \end{aligned} \quad (1)$$

where $H_y(z, t)$ and $E_x(z, t)$ represent the magnetic and electric fields propagating along the z direction, respectively, μ_0 and ϵ_0 are the magnetic permeability and electric permittivity of free space, respectively, N_{at} represents the density of polarizable atoms, Γ is the dipole coupling coefficient, T_1 is the excited-state lifetime, T_2 is the dephasing time, ω_{12} is the transition resonance angular frequency of the two level medium, and ρ_1 and ρ_2 are the real and imaginary components of the polarization –which determine the index of refraction and gain coefficients, respectively– [8]. The population difference is ρ_3 , and ρ_{30} represents its initial value.

As mentioned above, an hyperbolic secant two-color pulse, which can be expressed as

$$E_x(z=0, t) = E_\omega(t) + E_{3\omega}(t) = E_0 \operatorname{sech}((t-t_0)/t_p) \times [\cos(\omega(t-t_0)) + \cos(3\omega(t-t_0) + \phi)], \quad (2)$$

is externally injected to the system. The peak input electric field amplitude E_0 is chosen the same for both pulses and, in terms of the pulse area A , it is given by $E_0 = A\hbar/(\pi\Gamma t_p)$ [13]. The duration of the pulse is given by $t_p = \tau_p/1.763$, with τ_p being the full width at half maximum (FWHM) of the pulse intensity envelope. t_0 gives the offset position of the pulse center at $t=0$, and it is the reference value for the absolute phase of the pulses. The angular frequencies of the pulses are ω and 3ω , and ϕ is the relative phase. The parameters have been chosen as follows: $T_1 = T_2 = 1$ ns, $\tau_p = 10$ fs, $\Gamma = 2.65e\text{\AA}$, and $N_{at} = 2 \times 10^{18}$ cm $^{-3}$. It is important to note that our simulations give information on the coherent (transient) behavior of the system, since the dephasing time scales

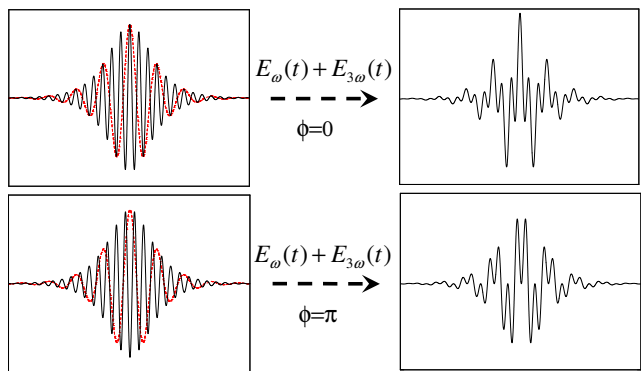


FIG. 2: Superposition of the electric field of the pulses. $E_\omega(t)$ is the electric field of the pulse with frequency ω represented as a function of time, and $E_{3\omega}(t)$ represents the pulse with frequency 3ω (see also Eq. (2)). As indicated, the upper figures correspond to the addition of the pulses in phase ($\phi = 0$), and the lower ones correspond to the addition out of phase ($\phi = \pi$).

are chosen much larger than the duration of the pulses $T_1, T_2 \gg \tau_p$.

Figure 2 is a representation of the electric field of the injected pulses. In the two upper figures we can observe the addition of two pulses with frequencies ω and 3ω in the case that the relative phase ϕ between them is $\phi = 0$. We note that the constructive interference in the center of the pulses results in a maximum of the resulting pulse (Fig. 2 upper-right), while in the case that the pulses are added out of phase ($\phi = \pi$), there is destructive interference in the center of the pulses and therefore the resulting pulse (Fig. 2 upper-right) presents a zero in the center. We will show below that the different shape, which only depends on the relative phase between the two $\omega - 3\omega$ pulses, is crucial in the nonlinear interaction with the two-level medium in the case of ultrashort intense pulses.

We next show the results of the simulations corresponding to the first scheme (Fig. 1) that we have analyzed. In Fig. 3, we represent the spectrum of the field for different positions of the propagation. The two highest peaks on the left of each spectra, in Fig. 3, correspond to the frequencies of the pulses initially injected to the medium ($\omega/2\pi$ and $3\omega/2\pi$). When the two pulses are initially in phase ($\phi = 0$), a third frequency (anti-Stokes) component is generated at $5\omega = 3\omega + (3\omega - \omega)$, as shown in Fig. 3(a). It is clear in that case that the conversion of the third harmonic component (3ω) to the 5ω -component [which is marked with a dotted arrow in Fig. 3(a)] increases as the propagation length increases. Differently, however, when the two pulses are initially out of phase ($\phi = \pi$), the conversion to the 5ω -component is completely suppressed, as it can be observed in Fig. 3(b). This contrasting behavior, to the best of our knowledge,

has not been observed before. We attribute this phenomenon to the dependence on the shape of the carriers (see Fig. 2) of the quantum interferences of the medium, which in the case of intense ultrashort pulses are governed by the electric field itself rather than by its envelope [9].

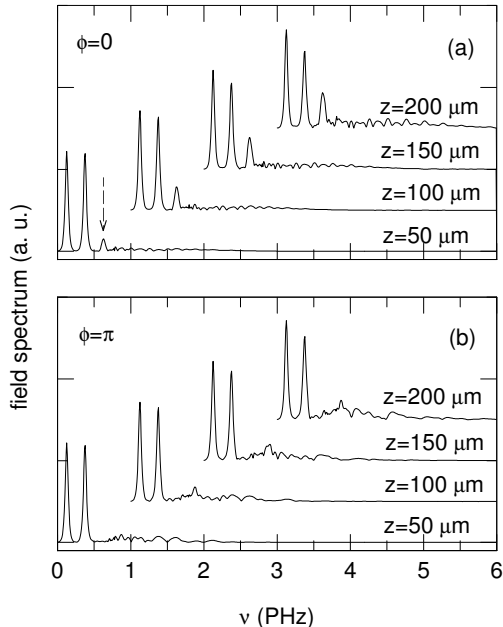


FIG. 3: Evolution of the field spectra as the pulses propagate through the two-level medium, as indicated. (a) $\phi = 0$; (b) $\phi = \pi$. The dotted arrow in (a) indicates the peak at frequency 5ω . The spectra have been shifted right and up for different z .

For longer propagation distances ($z \approx 500 \mu\text{m}$), the coupling between the fields will not longer be effective, because of changes in the shape of the pulses, as a consequence of the propagation effects, and also because of the progressive change in the spectral energy distribution of the field. In Fig. 4, we have plotted the spectra of the propagating field, in logarithmic scale, for propagation distances up to $z = 500 \mu\text{m}$. We can see how the usual higher spectral components are increasingly generated in the field as the propagation distance increases. These higher spectral components are due, on the one hand, to the interference between the pulses and the associated nonlinear processes [12], and on the other hand, to carrier-wave Rabi flopping phenomena which are present due to the high energies contained in the injected pulses [9]. As can be observed in Fig. 4(c), in the case of the present simulations, the spectrum spreads over the entire UV region for $z = 500 \mu\text{m}$. Note that some sensitivity on the initial relative phase ϕ of the spectra, in the higher frequency region, can also be observed in Fig. 4. Further details on these long propagation effects, however,

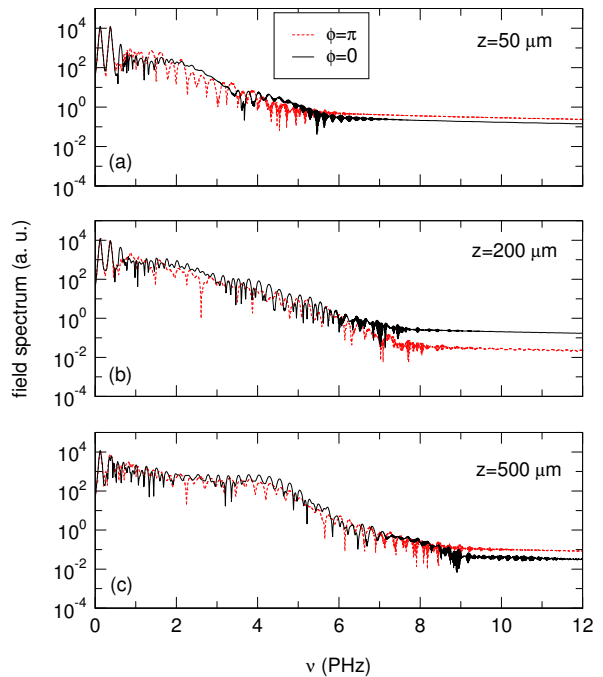


FIG. 4: Evolution of the field spectra as the pulses propagate through the two-level medium. (a) $z = 50 \mu\text{m}$; (b) $z = 200 \mu\text{m}$; (c) $z = 500 \mu\text{m}$. Note that the vertical axis is shown in logarithmic scale.

are left to be given elsewhere.

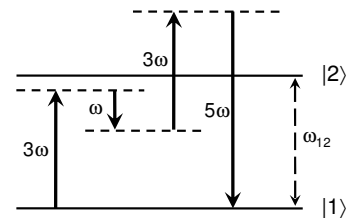


FIG. 5: Energy level scheme representing our second study. As in the previous scheme (1), the coupling can occur between the fields injected at frequencies ω and 3ω , and a third field generated at 5ω . The wavelengths associated to the frequencies in this scheme are: $\lambda_{(\omega)} = 1743 \text{ nm}$; $\lambda_{(3\omega)} = 581 \text{ nm}$; $\lambda_{(5\omega)} = 348.6 \text{ nm}$; $\lambda_{(\omega_{12})} = 580 \text{ nm}$. The area of the pulses is $A = 4\pi$. Note that, in this case, the field at 3ω is close to resonance with the transition of the medium.

The second energy level configuration that we have analyzed is represented in Fig. 5. In this case, two overlapping pulses with a duration of $\tau_p = 10 \text{ fs}$ are injected to the two-level medium. The area of the pulses is in that case much smaller ($A = 4\pi$) than in the previous scheme, and the field at frequency 3ω is now nearly in resonance with the transition of the medium. In Fig. 6 the field spectra for two different positions are shown ($z = 50 \mu\text{m}$

[Fig. 6(a)] and $z = 300 \mu\text{m}$ [Fig. 6(b)]. We clearly observe that the transfer of energy to the 5ω -component (which is marked with a dotted arrow in Fig. 6) is only efficient in the case of constructive interference in the centre of the pulses ($\phi = 0$), while it is almost suppressed for ($\phi = \pi$). On the other hand, the rest of the main peaks in the spectra, which result from the interference of the fields, remain basically insensitive to the variations of ϕ , and we therefore conclude that the influence of the initial relative phase is mostly observed in the four-wave coupling to the 5ω -component. This second study hence provides another demonstration of the possibilities of the phase control phenomena that we report.

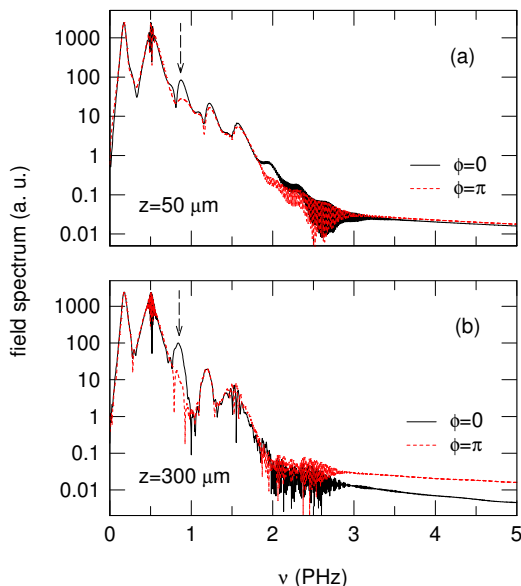


FIG. 6: Field spectra at $z = 50 \mu\text{m}$ (a) and $z = 300 \mu\text{m}$ (b). The dotted arrows indicate the peaks at frequency 5ω for $\phi = 0$.

We finally note that the results of the second scheme that we have investigated can be compared with previous work [7], where in a similar configuration the production of higher spectral components even for small pulse areas was demonstrated, and it was shown that the oscillatory structures around the resonant frequency and the propagation features of the laser pulses depend sensitively on the relative phase ϕ of the two pulses. We have here addressed the influence of the relative phase on the nonlinear coupling to the optical field at frequency 5ω , which was not considered in [7], and in that sense the second study in our work can be considered as complementary to that investigation.

In conclusion, we have analyzed the coherent propagation of two-color ω - 3ω femtosecond laser pulses overlapping in time and propagating in a two-level system to an extent of some hundreds of microns. Our study predicts

a critical dependence on the relative initial phase for the transfer of energy by four-wave mixing to the field at frequency 5ω . This effect is clearly observed in our simulations for propagation distances as long as $z \approx 300 \mu\text{m}$. We have observed this phenomenon in the case of highly intense femtosecond pulses strongly detuned from the transition of the medium, and also for pulses with moderate intensity close to resonance with the material transition. We have hence demonstrated that the manipulation of the initial absolute phase of the different frequency components of synchronously propagating ω - 3ω femtosecond pulses can serve as a means to control the nonlinear coupling to the optical field at frequency 5ω in four-wave mixing interactions. This coherent control can be useful, in particular, to limit the background nonresonant contributions in coherent anti-Stokes Raman processes.

Support from the *Programa Ramón y Cajal* of the Spanish Ministry of Science and Technology, from projects BFM2002-04369-C04-03 and FIS2004-02587, and from the Generalitat de Catalunya (project 2001SGR 00223), is acknowledged.

-
- [1] G. G. Paulus, F. Grasbon, H. Walther, P. Villorosi, M. Nisoli, S. Stagira, E. Priori, S. De Silvestri, *Nature* **414**, 182 (2001).
 - [2] E. Charron, A. Giusti-Suzor, and F. H. Mies, *Phys. Rev. Lett.* **71**, 692 (1993).
 - [3] S. Watanabe, K. Kondo, Y. Nabekawa, A. Sagisaka, and Y. Kobayashi, *Phys. Rev. Lett.* **73**, 2692 (1994).
 - [4] D. W. Schumacher, F. Weihe, H. G. Muller, and P. H. Bucksbaum, *Phys. Rev. Lett.* **73**, 1344 (1994).
 - [5] A. D. Bandrauk, N. H. Shon, *Phys. Rev. A* **66**, 031401(R) (2002);
 - [6] A. Brown, W. J. Meath, A. E. Kondo, *Phys. Rev. A* **65**, 060702 (2002);
 - [7] X. Song, S. Gong, S. Jin, and Z. Xu, *Phys. Lett. A* **319**, 150 (2003).
 - [8] R. W. Ziolkowski, J. M. Arnold, and D. M. Gogny, *Phys. Rev. A* **52**, 3082 (1995).
 - [9] S. Hughes, *Phys. Rev. Lett.* **81**, 3363 (1998).
 - [10] A. Taflov, *Computational electrodynamics: the finite-difference time-domain method*, Artech House Publishers, Boston-London (1995).
 - [11] A. V. Tarasishin, S. A. Magnitskii, and A. M. Zheltikov, *Optics Comm.* **193**, 187 (2001).
 - [12] See e.g., R. W. Boyd, M. G. Raymer, P. Narum, and D. J. Harter, *Phys. Rev. A* **24**, 411 (1981).
 - [13] J.-C. Diels and W. Rudolph, *Ultrashort laser pulse phenomena*, Optics and Photonics, Academic Press, San Diego (1996).
 - [14] J.-X. Cheng and X. S. Xie, *J. Phys. Chem. B* **108**, 827 (2004).
 - [15] M. Heid, T. Chen, U. Schmitt, and W. Kiefer, *Chem. Phys. Lett.* **334**, 119 (2001)
 - [16] D. Oron, N. Dudovich, D. Yelin, and Y. Silberberg, *Phys. Rev. A* **65**, 043408 (2002).